

NUMERICAL EXPERIMENTS
ON
CONTINENTAL LITHOSPHERE EXTENSION

by

JEREMY ROBERT HENDERSON

B.A., University of Oxford, England

(1980)

SUBMITTED IN PARTIAL FULFILLMENT
OF THE REQUIREMENTS FOR THE DEGREE OF
MASTER OF SCIENCE IN GEOPHYSICS
AT THE MASSACHUSETTS INSTITUTE OF TECHNOLOGY

May 1982

© MASSACHUSETTS INSTITUTE OF TECHNOLOGY

Signature of Author.
Department of Earth and Planetary Sciences

Certified by
Prof. J. G. Sclater
Thesis Supervisor

Accepted by.
Prof. T. Madden
Chairman, Department Committee

Uindgren
WITHDRAWN
JUL 1982
MIT LIBRARIES

NUMERICAL EXPERIMENTS ON CONTINENTAL LITHOSPHERE EXTENSION

by

JEREMY R. HENDERSON

Submitted to the Department of Earth and Planetary Sciences
on May 24, 1982 in partial fulfillment of the
requirements for the degree of Master of Science
at the Massachusetts Institute of Technology

ABSTRACT

The evolution of sedimentary basins is modelled by considering the extension of a thin viscous sheet of material with a temperature dependent power-law rheology subject to a constant velocity boundary condition, and introducing an initial strength perturbation with the system.

The degree of strain achieved in the weakened zone depends little on the magnitude of the initial strength perturbation, and greatly upon the rheology and stretching velocity assumed. The stretching in the weakened zone terminates when this zone has thinned sufficiently for mantle material to have risen near to the surface, cooled, and become strong again.

This model suggests why basins start to stretch, continue stretching for a period of time and then stop, with stretching starting elsewhere.

A rheology is considered in which the strain-rate is proportional to the n th power of the stress and to an exponential term involving an activation energy, Q .

When the value of Q/nRT_L (T_L is a reference temperature, which defines the initial geothermal gradient and R is the gas constant) is less than 20, the basin may take longer than 25 m.y. to form, and the post-rift subsidence will be less than 80% of that predicted by an instantaneous stretching model. Similarly, the surface heat flux is also less than predicted by an instantaneous stretching model.

These results suggest that a simple mechanical model of sedimentary basin formation can be used to explain a number of observed features of the strain history of basins, and that estimates of the thermal evolution of basins which do not take into account a realistic strain history may be seriously in error.

Thesis Supervisor: Dr. John Sclater

Title: Professor of Marine Geophysics

TABLE OF CONTENTS

	Page
TITLE PAGE	1
ABSTRACT	2
TABLE OF CONTENTS	3
1. INTRODUCTION	5
2. MANTLE RHEOLOGY AND CONSTITUTIVE RELATIONS	7
3. MODEL	
3.1 Physical Description	10
3.2 Mathematical Formulation	11
3.3 Parameter Range	19
4. RESULTS AND DISCUSSION	
4.1 Strain History	21
4.2 Heat Flow and Subsidence	24
5. CONCLUSIONS	28
ACKNOWLEDGEMENTS	30
REFERENCES	31
LIST OF FIGURES	33
LIST OF TABLES	36

"J'ai parlé d'une voix qui me disait ceci et cela. Je commençais à m'accorder avec elle à cette époque, à comprendre ce qu'elle voulait. Elle ne servait pas des mots qu'on avait appris au petit Moran, que lui à son tour avait appris à son petit. De sorte que je ne savais pas d'abord ce qu'elle voulait. Mais j'ai fini par comprendre ce langage. Je l'ai compris, je le comprends, de travers peut-être. La question n'est pas là. C'est elle qui m'a dit de faire le rapport. Est-ce à dire que je suis plus libre maintenant? Je ne sais pas. J'apprendrai. Alors je rentrais dans la maison et j'écrivais, Il est minuit. La pluie fouette les vitres. Il n'était pas minuit. Il ne pleuvait pas."

from "Molloy"

by Samuel Beckett

1. INTRODUCTION

McKenzie (1978) suggested that the main features of sedimentary basins could be explained in terms of a model in which isostatic subsidence during an instantaneous stretching event is followed by a period of thermally controlled subsidence during which geotherms, over-steepened during the stretching process, relax toward equilibrium.

These ideas have been applied to a variety of sedimentary basins, including the North Sea (Sclater and Christie, 1980), the Pannonian Basin (Sclater et al., 1980) and the Eastern U.S. continental margin (Sawyer et al., 1981). Estimates of the thermal evolution of a basin based on the assumption that stretching is instantaneous (McKenzie, 1978), or that it occurs at a constant strain rate (Jarvis and McKenzie, 1980), are handicapped because they construct a strain history using only total strain (McKenzie, 1978) or total strain plus duration of stretching (Jarvis and McKenzie, 1980). This results in an infinite strain rate, or a strain that increases exponentially with time, neither of which can be matched with boundary conditions usually considered appropriate for plate motions. Reconstructions of plate motions (for example Minster and Jordan, 1978) show that lithospheric plates move at roughly constant velocities for extended periods of time. It therefore seems more reasonable to assume that sedimentary basin formation results from lithosphere extension with a constant velocity boundary condition, rather than instantaneous or constant strain rate extension.

In order to model basin evolution more accurately, it is essential to understand the dynamic processes which operate during the stretching of continental lithosphere. In particular, it appears probable (see section 2) that the creep strengths of minerals in the lithosphere depend strongly

upon their temperature, and therefore the strain history may be strongly influenced by temperature changes which take place during lithosphere stretching (England, manuscript in preparation). The distribution of strength in the lithosphere is not well known, but the effects of temperature changes will be especially important if, as has been suggested (Brace and Kohlstedt, 1980) the strongest part of the lithosphere deforms by thermally activated creep of olivine.

Sedimentary basins observed in the geological record have many features, including failed rifts and outer highs, which indicate a complex strain history. To understand the significance of such observations we consider it important to discover which of these temporal variations may be consequences of the mechanical properties of the lithosphere when constrained by simple, geologically plausible boundary conditions, and which of them demand that we appeal to more exotic processes for an explanation. The dependence of hydrocarbon maturity on the stretching history of basins also provides a strong incentive for an inquiry into the dynamics of lithospheric stretching.

One of the first attempts to make a mechanical model of the process of sedimentary basin formation was by Vierbuchen et al. (in press). However, their approach has a number of drawbacks. First, they do not consider the changes in strength of the lithosphere produced by its thermal evolution. Their model is not really a thermo-mechanical model because they neglect the dependence of the mechanical evolution on the thermal evolution. Secondly, their constant-stress boundary condition leads to conclusions about the geometry of the deformed lithosphere which are hard to substantiate. Their model predicts that the weaker horizons in the lithosphere will end up longer than the strong horizons. It is hard to see

how this extra length can be accommodated in a realistic model of the Earth.

This thesis presents the results of a series of numerical experiments on a simpler mechanical model of the continental lithosphere than that chosen by Vierbuchen et al. The purpose of these experiments was not to simulate any real sedimentary basin, but to elucidate some of the mechanical effects of stretching a material with a temperature-dependent, power-law rheology over a parameter range large enough to encompass the full range of conditions believed likely to prevail in the lithosphere. We consider it important to understand these processes before moving on to more sophisticated models, and therefore we investigate a simple model which still allows us to draw useful conclusions about the evolution of sedimentary basins.

2. MANTLE RHEOLOGY AND CONSTITUTIVE RELATIONS

Realistic predictions about the mechanical behavior of a system can only be made by combining realistic boundary conditions and physical parameters with an appropriate constitutive relation. It is therefore important to review the constitutive relations believed to be applicable to the continental lithosphere.

Brace and Kohlstedt (1980) combine flow laws for quartz and olivine with the assumption that the upper crust fails by frictional sliding according to Byerlee's law to produce a tentative profile of strength of the lithosphere. If the crust deforms in a manner described by Byerlee's law and the assumed quartz flow law, then it is clear that the crust is much less strong than a mantle which deforms by plastic flow of olivine. Fig. 1 shows a typical strength profile resulting from these arguments, which is supported by studies of the distribution of seismicity in the lithosphere (Molnar and

Chen, in press). The work of Kusznir and Bott (1978) and Mithen (1982) suggests that modest tensional stresses applied to the whole lithosphere become concentrated in the crust, promoting failure by a brittle process such as normal faulting. We conclude that the most important region of the lithosphere in determining the strength is the mantle, particularly the uppermost mantle.

The conceptual framework within which most estimates of mantle rheology are made was defined by Stocker and Ashby (1973). These authors present a number of deformation maps which predict the flow of a material as functions of temperature, strain rate, differential stress etc. Different flow mechanisms require different stresses to maintain the same strain rate. The region of parameter space in which the lowest stress necessary to maintain a given strain rate is required by a particular mechanism is termed the "field" of that mechanism. The extents of these fields were predicted by Stocker and Ashby (1973) on the basis of the limited amount of available data, and by making estimates of the poorly constrained parameters by analogy with other materials. Fig. 2 shows one such deformation map taken from their paper, and also reproduced by Goetze (1978).

There has emerged a consensus of opinion that the dominant deformation mechanism in the upper mantle is some process involving the movement of dislocations. Practical considerations have limited experimental observations to strain rates of around 10^{-8} - 10^{-6} S^{-1} , whereas the mantle is believed to strain at rates of the order of 10^{-16} - 10^{-12} S^{-1} . Clearly, any extrapolation across the many orders of magnitude which separate experimental conditions from those prevailing in the mantle must be treated with caution. Also, Kirby (1980) presents evidence that at low temperatures (less than half the melting temperature) common earth materials may deform by transient creep, not the steady-state creep generally assumed.

Goetze (1978) reviews data including those which accumulated since 1973, and their effect on the predictions of Stocker and Ashby (1973). This review indicates that the data appear to correspond well to a combination of a 'power law' for differential stresses below about 2 kb and above this stress a relation of the type suggested by Dorn and Rajnak, 1964 (the Dorn Law), but the sparsity of data precludes a more deterministic analysis.

Goetze (1978) also indicates the possibility that a grain-size sensitive mechanism—Coble creep—may be important in low grain-size materials at high stress. The mathematical forms of these relations are

a) Power Law creep

$$\dot{\epsilon} = A(\sigma_1 - \sigma_3)^n \exp\left[\frac{-Q}{R\theta}\right]$$

b) Dorn Law creep

$$\dot{\epsilon} = \dot{\epsilon}_p \exp\left[-Q\left[1 - (\sigma_1 - \sigma_3)/\sigma_p\right]^2 R\theta\right]$$

c) Coble Creep (linear unless the grain-size is a function of stress)

$$\dot{\epsilon} = A(\sigma_1 - \sigma_3)^n \exp\left[\frac{-Q}{R\theta}\right]$$

The symbols used are explained in Table 1.

The values of A, n and Q are not necessarily the same in a), b), and c). The value of n probably lies in the range from 1 to 6, and the value of Q is almost certainly less than 200 kcal/mol, (Goetze, 1978).

If the available data were unambiguous and the relevant deformation mechanisms well understood, an extrapolation to geological strain-rates could be made with confidence. Unfortunately, this is not the case. The literature contains a wide variety of data obtained using a wide variety of experimental methods. Moreover, the non-equilibrium-thermodynamic nature of

dislocation creep makes it difficult to be certain that mechanisms postulated to occur in the laboratory are those which control the deformation of the mantle. It therefore seems desirable that any model which claims to represent upper mantle conditions should be investigated over a wide parameter range.

The constitutive relation chosen in this study is of the form of a power law, selected as being the best representation of the three relations mentioned earlier, and the parameter range is chosen to represent the uncertainty in experimental determinations and the assumptions inherent in a simplified mathematical model of this kind.

3. MODEL

3.1 Physical description

Before developing a detailed mathematical formulation of the model, it is valuable to present a preview of the processes which will be considered. The model has two uniform elements, side-by-side, which initially have the same thickness. Before stretching begins, we set the ratio of the lengths (L_1 and L_2) of these elements, and the ratio of the strengths (B_1 and B_2). The initially narrower element is, to start with, weaker, and for convenience we refer to it as the "basin". (Initial values are indicated by the superscript "0").

We then begin to extend the system. There is a simple relationship between the strengths of the elements and the element strain-rates resulting from a constant velocity boundary condition applied to the whole system. Given the strengths we can find the strain-rates and hence calculate the lengths of the elements after an increment of time has elapsed, and also the thicknesses.

Knowing the strain-rate history of the elements we can find the Moho temperatures, which, as we shall see, are the most important parameters in determining the strength of the element. Since we now again know the strengths and lengths of both elements we can repeat this procedure many times, obtaining a detailed picture of the strain history of the system. This method is shown schematically in Figure 3.

We may anticipate that the initially weaker element begins to strain very rapidly, but, as it thins, the insulating layer of crust which separates the atmosphere or sea from the strength-controlling uppermost mantle is attenuated, and therefore the element becomes more rigid. Eventually this, initially, weaker, element may "lock up" and the strain will be accommodated in the element which was initially stronger.

3.2 Mathematical formulation

We model the continental lithosphere as a thin sheet of viscous material with a temperature-dependent power-law rheology which is considered to strain in the vertical dimension and one horizontal dimension. The model has two elements, horizontally adjacent, one of which is initially weaker and narrower and is regarded as representing the incipient sedimentary basin. The elements initially have strengths B_1^0 and B_2^0 ($B_1^0 > B_2^0$) and lengths L_1^0 and L_2^0 ($L_1^0 > L_2^0$). The ends of the system are constrained to recede from one another at a constant velocity U_0 (Fig. 3). It is not our intention to suggest how the initial weakness might be induced, but likely candidates are pre-existing irregularities in the thickness of the lithosphere, and transient heat sources in the asthenosphere.

The motion of a viscous fluid in a stress field is described by the Navier-Stokes equation, which, neglecting body forces, and where rates of flow are small enough to justify ignoring acceleration terms, becomes

$$\frac{\partial p}{\partial x_i} = \frac{\partial \tau_{ij}}{\partial x_j} \quad (3.1)$$

where p is the pressure in the field and τ_{ij} the elements of the deviatoric stress tensor, and we use the convention of summing over repeated subscripts. Since we approximate the continental lithosphere by a thin viscous sheet with no strain in one horizontal dimension, then if there is no shear stress on the top or bottom of the lithosphere we may assume that there are no vertical gradients of horizontal velocity within it

($\dot{\epsilon}_{xz} = \dot{\epsilon}_{yz} = \dot{\epsilon}_{zx} = \dot{\epsilon}_{zy} = 0$) and so $\dot{\epsilon}_{xx} = -\dot{\epsilon}_{zz}$ and equation 3.1 reduces to

$$\frac{\partial p}{\partial x} = \frac{\partial \tau_{xx}}{\partial x} \quad (3.2)$$

In this formulation, pressure gradients arise from gradients in crustal thickness (England and McKenzie, in press) and we assume that the magnitude of these gradients is not sufficient to affect the deformation. Neglecting horizontal gradients of pressure we have

$$\frac{\partial \tau_{xx}}{\partial x} = 0 \quad (3.3)$$

The assumption that the deformation within the lithosphere is independent of depth ($\dot{\epsilon}_{xz} = 0$) means that we ignore the role of brittle deformations. Since faults represent only the fracture of a thin brittle layer, and not the deformation of the whole lithosphere this is not unreasonable. For the purpose of this study we regard faults as a consequence of the viscous deformation of the lithosphere, and not as a controlling mode of deformation in themselves (see also section 2). Also, the nature of faulting in a given region certainly owes something to the regional fabric which results from previous tectonic events, and therefore a model such as this cannot predict

a particular location or type of faulting, though it can predict the general stress regime.

We therefore need to consider the vertically averaged stress within the lithosphere. This is given by $\frac{1}{d} \int_0^d \tau_{xx} dz$, where the lithosphere has initial thickness d . We have already discussed the rationale for using a power law constitutive relation of the form

$$\dot{\epsilon} = A(\sigma_1 - \sigma_3)^n \exp \left[\frac{-Q}{R\theta} \right] \quad (3.4)$$

This equation, appropriate for the case of uniaxial stress and strain, may be generalized by the introduction of the second invariant of the deviatoric stress tensor, $T = (\tau_{ij} \tau_{ij})^{1/2}$, or the second invariant of the strain-rate tensor, $\dot{E} = (\dot{\epsilon}_{ij} \dot{\epsilon}_{ij})^{1/2}$, thus:

$$\dot{\epsilon}_{ij} = CT^{n-1} \tau_{ij} \exp \left(\frac{-Q}{R\theta} \right) \quad (3.5)$$

Since $\epsilon_{xx} = -\epsilon_{zz}$ and the other elements of the strain rate tensor are zero, these second invariants are simply $T = \sqrt{2} |\tau_{zz}|$ and $\dot{E} = \sqrt{2} |\dot{\epsilon}_{xx}|$, so

$$\dot{\epsilon}_{xx} = D \tau_{xx}^n \exp \left(-\frac{Q}{R\theta} \right) \quad (3.6)$$

or

$$\tau_{xx} = D^{-1/n} \dot{\epsilon}_{xx}^{1/n} \exp \left(\frac{Q}{nR\theta} \right) \quad (3.7)$$

The vertically averaged stress is therefore

$$\frac{1}{d} \int_0^d \tau_{xx} dz = F \dot{\epsilon}_{xx}^{1/n} \int_0^d \exp(Q/nR\theta) dz \quad (3.8)$$

And if we assume that the stress required to deform the crustal lithosphere is much less than that required to deform the mantle lithosphere, and that

there is a linear geotherm: $\theta(z) = \theta_0 + gz$ where θ_0 is the surface temperature then equation (3.8) becomes

$$\frac{1}{d} \int_0^d \tau_{xx} dz \approx \frac{F \dot{\epsilon}_{xx}^{1/n}}{g} \frac{T_L}{\theta_m} \int \exp\left(\frac{Q}{nR\theta}\right) d\theta \quad (3.9)$$

For $Q/nR > 5$ and $\theta_L \gg \theta_m$, this may be solved approximately, giving

$$\frac{1}{d} \int_0^d \tau_{xx} dz \approx \frac{\dot{\epsilon}^{1/n} F n R \theta_m^2}{g Q} \exp\left(\frac{Q}{nR\theta_m}\right) \quad (3.10)$$

i.e.
$$\tau_{xx} = B \dot{\epsilon}_{xx}^{1/n} \quad (3.11)$$

where
$$B = \frac{F n R \theta_m^2}{Q g} \exp\left(\frac{Q}{nR\theta_m}\right) \quad (3.12)$$

The quantity $\frac{F n R}{Q}$ is a constant for the material, hence

$$B \propto C \frac{\theta_m^2}{g} \exp\left[\frac{Q}{nR\theta_m}\right] \quad (3.13)$$

Equation (3.10) may also be written in terms of the second invariant of the strain-rate tensor:

$$\frac{1}{d} \int_0^d \tau_{xx} dz = F \dot{\epsilon} \dot{\epsilon}^{1/n-1} \frac{nR\theta_m}{Q} \frac{\theta_m}{g} \exp\left(\frac{Q}{nR\theta_m}\right) \quad (3.14)$$

This linear relation between the stress and strain rate contains a scale effective viscosity, $\dot{\epsilon}^{1/n-1} \exp\left(\frac{Q}{nR\theta_m}\right)$ and a scale depth $\frac{nR}{Q} \frac{\theta_m}{g}$.

The strain rate history of our model system is controlled by two opposing effects: a) As the lithosphere stretches it becomes weaker, and b) as the thinning proceeds, material in the strongest layer is carried towards the surface, cools, and becomes still stronger.

The degrees of stretching of the two elements of the model are β_1 and β_2 , where

$$\beta_1 = \frac{L_1}{L_1^0} \quad (3.15)$$

and

$$\beta_2 = \frac{L_2}{L_2^0} \quad (3.16)$$

The ends of the system are constrained to recede from one another at a constant velocity U_0 . The strain rates of the element are $\dot{\epsilon}_1$ and $\dot{\epsilon}_2$ and the constant velocity boundary condition corresponds to an initial bulk strain rate of

$$\dot{\epsilon}_0 = \frac{U_0}{L_1^0 + L_2^0} \quad (3.17)$$

which, for $\frac{L_1^0}{L_2^0} \gg 1$ is approximately

$$\dot{\epsilon}_0 = \frac{U_0}{L_1^0} \quad (3.18)$$

Since there are no horizontal gradients of stress, we have:

$$B_1 \dot{\epsilon}_1^{1/n} = B_2 \dot{\epsilon}_2^{1/n} \quad (3.19)$$

and from the boundary condition:

$$L_1 \dot{\epsilon}_1 + L_2 \dot{\epsilon}_2 = U_0 \quad (3.20)$$

Eliminating $\dot{\epsilon}_1$ from (3.19) and (3.20) we find $\dot{\epsilon}_2$ is given by:

$$\dot{\epsilon}_2 = \frac{\dot{\epsilon}_0 / \beta_2}{\left[\frac{L_1}{L_2} \left(\frac{B_2}{B_1} \right)^n + 1 \right]}$$

and hence $\dot{\epsilon}_1$ is found from (3.19) by:

$$\dot{\epsilon}_1 = \dot{\epsilon}_2 \left(\frac{B_2}{B_1} \right)^n \quad (3.21)$$

After m time-steps of finite length δt , β_1 and β_2 are found from

$$\beta_1 = 1 + \sum_{i=1}^m \dot{\epsilon}_1(i-1) \delta t \quad (3.22)$$

and

$$\beta_2 = 1 + \sum_{i=1}^m \dot{\epsilon}_2(i-1) \delta t \quad (3.23)$$

Equations (3.19) through (3.21) show that from given values of $\frac{L_1}{L_2}$, $\frac{B_2}{B_1}$

and $\dot{\epsilon}_0$ we can progressively calculate the strain history of the system, timestep by timestep, provided we know the Moho temperature of both elements, in order to calculate new values of $\frac{B_2}{B_1}$.

This differs from the approach used by England (in prep.), in which the velocity boundary conditions were applied to a homogeneous lithosphere, with the result that the strain rate within the lithosphere always obeyed the relation:

$$\dot{\epsilon}(t) = \dot{\epsilon}_0 / \beta \quad (3.24)$$

or
$$\beta = 1 + \dot{\epsilon}_0 t \quad (3.25)$$

To find the Moho temperature precisely would entail solving the heat flow equation for each timestep, for both elements. Instead, we separate the mechanical and thermal problems, and to solve the latter we construct, from numerical solutions to eq. 3.26, a table of Moho temperatures and surface heat flux for increasing values of β , and various initial strain rates, for a homogeneous lithosphere undergoing extension with a constant velocity boundary condition and make the assumption that the solution to the thermal problem obtained for this situation is sufficiently accurate as long as the predicted strain history does not deviate too strongly from a simple constant velocity boundary condition extension. (This approximate solution was checked by calculating the exact solution for a number of cases, and was demonstrated to be sufficiently accurate for our purpose.) The thermal state of such a system is dependent upon the period of stretching, Δt , and the stretching factor, β . The model strain rate, $\dot{\epsilon}$, is related to the initial strain rate, $\dot{\epsilon}_0$, by equation (3.24), and the appropriate non-dimensional heat flow equation for this situation is

$$\frac{\partial T'}{\partial t'} + \dot{\epsilon}'(1-z') = \frac{\partial T'}{\partial z'} \frac{\partial^2 T'}{\partial z'^2} \quad (3.26)$$

where the non-dimensional time, t' is related to the dimensional quantity, t , by $t' = \kappa t / a^2$, κ and a being the thermal diffusivity and thickness of the lithosphere, and the non-dimensional depth, z' , is given by $z' = z/a$. The temperature is non-dimensionalised using the absolute undisturbed temperature at the base of the lithosphere, T_L , i.e. $T' = \theta / T_L$ (for comparison, see Jarvis and McKenzie, 1980, equation 2), or England, in prep., equation 8). Hence the non-dimensional strain rate is related to the dimensional strain rate by

$$\dot{\epsilon}' = \frac{a^2}{\kappa} \dot{\epsilon} \quad (3.27)$$

$$\text{or} \quad \dot{\epsilon}' = \frac{Pe/\kappa}{a^2 \beta} \quad (3.28)$$

where Pe is the Peclet number for the system, which is also given by

$$Pe = \frac{\dot{\epsilon}_0 a^2}{\kappa} \quad (3.29)$$

$$\text{or} \quad Pe = \frac{(\beta-1)\kappa}{a^2 \Delta t} \quad (3.30)$$

where Δt is the period of stretching. Since we know β for both elements, and we know the period of stretching, we can easily find what the initial strain rate, would have been if the elements had each undergone extension at a constant velocity. By using these values of β and $\dot{\epsilon}_0$, and interpolating linearly between values of Moho temperature given in the table referred to above, we can arrive at an approximation to the Moho temperature which will be accurate if the strain histories of both the elements approximate to a constant velocity extension.

The strength of an element, B_k ($k = 1, 2$) is related to its Moho temperature, θ_m and geothermal gradient, g by equation (3.12)

$$B_k \propto \frac{1}{g} \theta_m^2 \exp\left(\frac{Q}{nR\theta_m}\right) \quad (3.31)$$

If the initial strength, B_k° is related to the initial Moho temperature, T_0 , and geothermal gradient g_0 , then

$$B_k^\circ \propto \frac{1}{g_0} T_0^2 \exp\left(\frac{Q}{nRT_0}\right) \quad (3.32)$$

and

$$\frac{B_k}{B_k^\circ} = \frac{g_0}{g} \left(\frac{\theta_m}{T_0}\right)^2 \exp\left[\frac{Q}{nR} \left(\frac{1}{\theta_m} - \frac{1}{T_0}\right)\right] \quad (3.33)$$

Now, if we note that $g/g_0 = \beta$, and non-dimensionalize the temperature with respect to the temperature at the base of the lithosphere, T_L i.e.

$\theta_m = \theta_m' \cdot T_L$ and $T_0 = T_0' \cdot T_L$ equation (3.32) becomes

$$\frac{B_k}{B_k^\circ} = \frac{1}{\beta} \left(\frac{\theta_m'}{T_0'}\right)^2 \exp\left[\frac{Q}{nRT_L} \left(\frac{1}{\theta_m'} - \frac{1}{T_0'}\right)\right] \quad (3.34)$$

Equation (3.34) shows that the strength of an element, relative to its initial strength, depends exponentially upon the ratio Q/nRT_L , and suggests that Q/nRT_L can profitably be considered as a single parameter.

3.3 Parameter Range

All the experiments reported below were begun by assuming an initial length ratio of $\frac{L_1^\circ}{L_2}$ of 10 and an initial viscosity contrast $\frac{B_2^\circ}{B_1}$ ranging from 0.01 to 0.75. We consider initial non-dimensional strain rates of between 5

and 150. Using a value of $\frac{a^2}{\kappa}$ of 625 m.y., quoted by Parsons and Sclater (1977) as being appropriate to the oceanic lithosphere this is equivalent to strain rates from $2.5 \times 10^{-16} \text{ s}^{-1}$ to $8 \times 10^{-15} \text{ s}^{-1}$. Over the range of temperatures prevailing in the lithosphere - probably less than 1700 K, these strain-rates fall within the Coble-creep and dislocation creep fields of Stocker and Ashby (1973) (see Fig. 2).

It is necessary to use a large range of activation energies, since activation energy is one of the least well-determined parameters in the constitutive relation. Since the temperature at the base of the lithosphere is also poorly constrained we consider the single parameter Q/nRT_L to vary widely, between 1.5 and 40. For a value of $T_L = 1500 \text{ K}$, if the gas constant, R , is 2 cal/mol and the value of n is 3, a Q/nRT_L of 10 corresponds to an activation energy of 90 kcal/mol. Similarly, for a Newtonian lithosphere ($n=1$) with a temperature at the base of the lithosphere of 1500 K, Q/nRT_L of 40 corresponds to an activation energy of 120 kcal/mol. Values of n between 1 and 6 are considered.

For Q/nRT_L as high as 40, the only value of n which gives a reasonable activation energy is $n = 1$. Therefore we shall, in general, consider that $Q/nRT_L = 40$ corresponds to a Newtonian lithosphere.

The quantitative results reported below were derived only from those numerical experiments for which the temperature estimate was demonstrated to be accurate, i.e. when the calculated strain histories were reasonably close to a constant velocity extension.

4. RESULTS AND DISCUSSION

4.1 Strain History

Over the entire parameter range the strain rate history of the system shows the general form depicted in Fig. 5 . The weaker zone stretches very rapidly and, as it becomes thinner, the effective viscosity decreases, concentrating the strain. However, this rapid thinning is not maintained because mantle material is brought closer to the surface, cools, and becomes stronger until eventually, the pre-weakened zone, which, for convenience we will refer to as the "basin" begins to "lock up", and the strain is taken up by the rest of the continent. This results in the length-ratio profile shown in Fig. 6.

One of the principal features of interest is the degree of concentration of strain into the basin region which can be achieved during stretching. It is therefore of interest to find the strain in the basin, at the time of the maximum concentration of strain, that is, to find β_2 when $\dot{\epsilon}_1 = \dot{\epsilon}_2$ (and $\frac{L_1}{L_2}$ is a minimum).

Figs 7, 8 and 9 show contours in $Q/nRT_L - \dot{\epsilon}_0$ space of β_2 at the time when $\dot{\epsilon}_1 = \dot{\epsilon}_2$ for different values of B_2^0/B_1^0 . We do not show contours where β_2 is greater than ten, because it seems likely that by that stage large-scale intrusions would significantly influence the stretching process (Le Pichon and Sibuet, 1981, argue that such intrusion is likely to begin when the stretching factor is as little as 3 or 4) and render our model inapplicable. Neither do we plot any values for stretching during which the stress in the system exceeds twenty-five times the initial value, because this would represent such a large departure from the initial conditions that

processes other than those modelled here would probably begin to play an important role. The effect of the latter condition is to eliminate β_2 values for $B_2^0/B_1^0 = 0.01$ when n is 3 or 6. Since the time when $\dot{\epsilon}_1 = \dot{\epsilon}_2$ is also the time when the two elements have the same strength, then when stretching takes place too quickly for B_1 to change significantly from B_1^0 , the strength of the basin must increase by a factor of about B_1^0/B_2^0 before $\dot{\epsilon}_1 = \dot{\epsilon}_2$. These conditions prevail for $B_2^0/B_1^0 = 0.01$ and $n = 3$ or 6. When $n = 1$, the strengthening of the basin is accompanied by a weakening of the rest of the continent, and the stress in the system does not increase as rapidly as when n is 3 or 6.

One of the most important points which is made clearly by figures 7 to 9 is that the disposition of β_2 contours in $Q/nRT_L - \dot{\epsilon}_0$ space is not significantly altered by making large changes in the value of B_2^0/B_1^0 , the initial strength contrast. The largest stretching factor possible for the maximum initial strain rate when $Q/nRT_L = 40$ varies only from 3 to 4.5 as the value of B_2^0/B_1^0 ranges over nearly two orders of magnitude. The range of parameter space where a β_2 of greater than 10 is possible also varies relatively little over a wide range of B_2^0/B_1^0 . The reason for this is made apparent by considering a plot of the stress in the system (relative to its initial value) against β_2 - an example is shown in Figure 10. As we have already noted, $\dot{\epsilon}_1 = \dot{\epsilon}_2$ when the initial strength contrast has been evened out by the strengthening of the basin and the weakening of the rest of the continent, and at this the point the ratio τ/τ_0 is roughly equal to (B_1^0/B_2^0) , that is to say, $\dot{\epsilon}_1 = \dot{\epsilon}_2$ when τ/τ_0 increases to some value which depends upon B_2^0/B_1^0 and, to a lesser extent, upon the strain history. Figure 10 shows that a large change in the value of τ/τ_0 takes place over a small range of β_2 , when the effect of cooling on the strength of the

lithosphere is most marked, and therefore that the value of β_2 when $\dot{\epsilon}_1 = \dot{\epsilon}_2$ is not strongly dependent upon the initial strength contrast. The value of β_2 when this rapid increase in the strength of the lithosphere takes place depends on the initial bulk strain rate and the sensitivity of the strength of the lithosphere to temperature changes i.e. on the values of n and Q . It is the relative importance of n , Q and $\dot{\epsilon}_0$ in determining the disposition of the β_2 that can be seen in Figures 7-9.

For a small boundary velocity (i.e. a small initial strain rate), changing Q/nRT_L by a factor of two can have a dramatic effect on the strain concentration. For example, when $B_2^0/B_1^0=0.75$ (Fig. 9) and $\dot{\epsilon}_0$ is 5, increasing Q/nRT_L by a factor of two leads to a decrease in the value of β_2 by a factor of five, from 10 to 2. The effect of changing Q/nRT_L is much less important at higher strain rates.

Though our model can only describe, at best, the behaviour of a continental lithosphere during the initial phase of a single purely extensional event, it may be profitable to speculate upon the geological implications of our results. It appears from these figures that unless the stretching velocity, the temperature at the base of the lithosphere or the power law exponent is large, or the activation energy for lithosphere deformation is small, it is unlikely that a piece of continental lithosphere can be stretched continuously until a large degree of thinning is achieved and oceanic crust formed. In fact, the margins of major oceans are marked by evidence of multiple phases of stretching and quiescence, indicating that stretching, cooling and "locking up" of continental lithosphere may play a significant role in determining the strain history of an extensional province. For a value of Q/nRT_L of 40, corresponding to the Newtonian lithosphere, and a range of realistic strain rates, this "locking up"

appears to take place when β_2 is around 1.5, or a stretching of 50%. This figure corresponds well with estimates of the degree of stretching of a number of well-documented sedimentary basins. For example, Sclater and Christie quote values of around 50% for the amount of stretching which has taken place in the central North Sea. It is also in accordance with the estimates of the maximum possible stretching made using simpler models (England, 1981). Clearly our model is far too crude to use as a basis for predicting actual amounts of stretching, but it is encouraging that the results do not differ widely from reasonable values, and lends support to the idea that cooling and strengthening of the lithosphere is a probable extension-inhibiting process.

4.2 Heat flow and subsidence

An important factor in determining hydrocarbon maturity is the surface heat flow during stretching. For this reason we include a brief discussion of the implications of our stretching model to the thermal evolution of the lithosphere, bearing in mind the caveat mentioned in section 4.1 -that we are only using an approximate solution to the thermal problem.

In spite of this, it is possible to make some important observations on the dependence of the thermal history on the model parameters. Figs. 11 to 13 show the surface heat flux plotted against the stretching factor, β_2 , for $B_2^0/B_1^0 = 0.1$ and n is 1, 3 and 6. McKenzie's (1978) model predicts that when stretching stops the heat flow will lie on the line $q/q_0 = \beta$, at the appropriate value of β . This is clearly not the case for a model which includes finite strain rates. In fact, the peak in the q/q_0 curve is significantly displaced from the $q/q_0 = \beta$ line.

In order to compare the post-rift subsidence predicted by this model with that predicted by the instantaneous uniform extension model we consider

the situation depicted in Fig. 14. Immediately stretching ceases the lithosphere, of initial thickness a , has a thickness of a/β . At a depth z it has a temperature $\theta^\circ\text{C}$ and hence a density $\rho = \rho_0(1-\alpha\theta(z))$, where ρ_0 is the density at 0°C and α is the thermal expansivity. The surface is maintained at 0°C and the temperature below a depth a is $T_L^\circ\text{C}$. The geotherm is $\theta(z)$, and for $z < a$ this is, in general, non-linear. This column of material is isostatically compensated at a depth of $s+a$. The lithosphere subsides after stretching by a distance s , and is covered by a column of seawater of height s with density ρ_w , and the lithosphere geotherm is linear. Isostasy requires that the columns in 14a) and 14b) have the same mass, i.e.

$$\rho_0 \int_0^a (1-\alpha\theta(z))dz + s\rho_0(1-\alpha T_L) = s\rho_w + a\rho_0(1-\alpha\frac{T_L}{2}) \quad (4.1)$$

hence

$$s = \frac{a(1 - \frac{\alpha T_L}{2}) - \int_0^a (1-\alpha\theta(z))dz}{((1-\alpha T_L) - \frac{\rho_w}{\rho_0})} \quad (4.2)$$

If the stretching had occurred instantaneously, the value of the integral

is simply $a - a\alpha T_L + \frac{a\alpha T_L}{2\beta}$

and

$$s = \frac{a\alpha T_L}{2((1-\alpha T_L) - \rho_w/\rho_0)} \gamma \quad (4.3)$$

where $\gamma = 1 - 1/\beta$

The form of this solution suggests that we express the solution to the general problem as

$$s = \frac{a\alpha T_L}{2((1-\alpha T_L) - \rho_w/\rho_o)} \gamma^* \quad (4.4)$$

where γ^* is a function of the temperature profile, which depends upon β and the strain history. This temperature profile is supplied by the same program which supplied the Moho temperatures and surface heat fluxes, so we can find γ^* at the time of maximum heat flux for a variety of rheologies and initial strain-rates. The values of γ and the ratio γ^*/γ obtained are presented in Table 2.

Table 2 also gives the value of the ratio of the stress in the system to its initial value, τ/τ_o , at the time of maximum heat flux. Using this table in conjunction with figs. 11-13 we can draw a number of important conclusions about the influence of rheology and initial strain rate on the thermal and subsidence history of a sedimentary basin.

First of all, it is clear that the form of the heat flow profiles in figs. 11-13 depends little on the value of n , and strongly upon the initial strain-rate and the ratio Q/nRT_L . The time of maximum heat flux corresponds well to the time when the basin begins to "lock up" and the value of the maximum heat-flux is greatest for those rheologies which allow stretching to take place rapidly, i.e. the lower the activation energy, or the higher the initial strain rate, the greater will be the oversteepening of the geotherm before significant strengthening can occur, and hence the higher the heat flux. When ϵ_o is 150 the maximum heat flux varies from 3 ($Q/nRT_L = 40$) to 5.5 ($Q/nRT_L = 1.5$) whereas for slow stretching, with $\dot{\epsilon}_o = 5$, the maximum heat flux is confined to the range between 1.2 ($Q/nRT_L = 40$) and 1.5 ($Q/nRT_L = 1.5$).

From the values of τ/τ_0 at the time of maximum heat flux (Table 2) it is apparent that for Q/nRT_L , τ/τ_0 is low, typically around 0.5, but for higher Q/nRT_L this ratio of stresses is high, suggesting that stretching may have been halted before the curve has departed greatly from the $q/q_0 = \beta$ line, and that such a basin may be difficult to distinguish from a basin which has stretched instantaneously.

There is no such systematic relationship between τ/τ_0 and the initial strain rate because although high strain rates require large stresses for a given lithosphere strength (see equation 3.11), low strain rates permit thermal relaxation and "locking up" of the basin. Which of these processes dominates depends on the value of the power-law exponent—high values of n acting to promote the former effect. Hence, for $n=3$, increasing initial strain rate is accompanied by an increase in τ/τ_0 for a given Q/nRT_L . For $n=1$ higher strain rates result in lower τ/τ_0 . When $n=6$, whether τ/τ_0 increases or decreases with strain rate depends upon the value of Q/nRT_L .

The amount of post-rift subsidence predicted by this model is significantly less than that predicted by McKenzie's (1978) model for the case of instantaneous stretching (and, by implication, the syn-rift subsidence is greater). This difference is most marked for low initial strain rates, which cause a slow stretching, since the long stretching time allows significant syn-tectonic thermal relaxation to take place. The ratio γ^*/γ varies from around 0.5 for $\dot{\epsilon}_0 = 5$ to around 0.85 for $\dot{\epsilon}_0 = 150$. Rheologies which bring stretching to a halt rapidly, i.e. high Q/nRT_L , allow little time for thermal relaxation and hence γ^*/γ is higher for higher values of Q/nRT_L .

The value of γ^*/γ depends, therefore, upon the time taken to achieve the maximum surface heat flux. Comparing these values of γ^*/γ with the

dimensionless time taken to reach maximum heat flux reveals that γ^*/γ is less than 0.8 for dimensionless times of about 4×10^{-2} DTU. For a lithosphere with $a^2/\kappa = 625$ m.y. (Parsons and Sclater, 1977) this corresponds to time of 25 million years, that is to say that a basin taking 25 million years to achieve maximum heat flux will have a post-tectonic subsidence which is only 80% of that predicted for a basin formed by instantaneous stretching. Estimates of the thermal history for basins taking much longer than 25 m.y. to form may therefore be in error.

The shaded areas on Fig. 7, 8 and 9 show the region of parameter space in which basin stretching ceases at a time of 0.04 D.T.U. In the parameter space above the line, the stretching ceases in less than 0.04 DTU. These figures show that if Q/nRT_L is below about 20, then basin stretching will not be impeded by syn-deformation cooling and strengthening of the lithosphere for 25 million years.

5. CONCLUSIONS

A number of important points arise from modelling sedimentary basin formation as a consequence of extending a thin viscous sheet of a power-law material. First, and most important, there appears to be a limit on the amount of extension possible before the strong material in the "basin" portion of the lithosphere cools and strengthens, which does not depend strongly upon the initial strength contrast between the "basin" and the "continent". The amount of strain concentration achieved is determined by the velocity of extension and by the values of the parameters in the constitutive relation. The time-dependence of the locus of stretching indicates that tensional regimes may have a complex strain history which derives solely from the mechanical properties of the lithosphere.

The heat flow and post-rift subsidence predicted by this model are less than predicted by McKenzie's instantaneous stretching model. If the lithosphere has a Q/nRT_L of less than 20 then "locking up" is not likely to occur in less than 25 million years. If Q/nRT_L is greater than 20 it appears that sedimentary basins cannot stretch for periods of time longer than 25 million years. The fact that there are examples of basins which stretch for long periods of time suggests that, locally at least, the lithosphere is not Newtonian.

Basins taking longer than 25 million years to form subside after stretching less than 80% of the amount predicted by an instantaneous stretching model. Jarvis and McKenzie (1980) have already pointed out that the thermal state of a basin stretching for over 20 million years is significantly different from an instantaneously stretched basin. What we are now able to do is to show that stretching over a long period of time is not possible if the lithosphere behaves as a Newtonian fluid. Results such as these suggest that it may be important to consider the dynamic processes of basin formation when modelling thermal evolution, and that an assumption of instantaneous stretching may result in errors in estimates of hydrocarbon maturity.

Acknowledgements

I am very grateful to Phil England for the very considerable amount of help and advice he gave me throughout this work, and for his comments, both solicited and unsolicited.

I would also like to thank John Sclater, not only for reading and discussing (and signing!) this thesis but also for his enthusiastic support during my brief career at M.I.T.

I used the Harvard MTM system with the permission of Adam Dziewonski, Dorothy Frank speedily and efficiently typed the manuscript and Lee Mortimer kept the wheels of organization turning smoothly.

The impetus to start this investigation, and the funding to complete it, were provided by Exxon Production Research Company.

REFERENCES

- Brace W.F. and D.L. Kohlstedt, 1980, "Limits on lithospheric strength imposed by laboratory experiments", J. Geophys. Res., 85, 6248-6252.
- Dorn, J.E. and S. Rajnak, 1964, "Nucleation of kink pairs and the Peierls' mechanism of plastic deformation", Trans. AIME 230, 1052-1064.
- England, P.C., 1981, "Constraints on continental lithosphere extension", EOS, (Abstract) 62, p. 1022.
- England, P.C. and D.P. McKenzie, 1982, "A thin viscous sheet model for continental deformation", Geophys. J. R. astr. Soc., in press.
- Goetze, C., 1978, "The mechanisms of creep in olivine", Phil. Trans. R. Soc. Lond., A 288, 99-119.
- Jarvis, G.T. and D.P. McKenzie, 1980, "Sedimentary basins formation with finite extension rates", Earth Planet. Sci. Lett., 48, 42-52.
- Kirby, S.H., 1980, "Tectonic stress in the lithosphere: constraints provided by the experimental deformation of rocks", J. Geophys. Res., 85, 6353-6363.
- Kusznir, N.J. and M.H.P. Bott, 1977, "Stress concentration in the upper lithosphere caused by underlying visco-elastic creep", Tectonophysics, 43, 247-256.
- LePichon, X. and J.C. Sibuet, 1981, "Passive margins: a model of formation", J. Geophys. Res., 86, 3708-3721.
- McKenzie, D.P., 1978, "Some remarks on the development of sedimentary basins", Earth Planet. Sci. Lett., 40, 25-32.
- Minster, J.B. and T.H. Jordan, 1978, "Present day plate motions", Geophys. Res., 83, 5331-5354.
- Mithen, D.P., 1982, "Stress amplification in the upper crust and the development of normal faulting", Tectonophysics, 83, 259-274

- Molnar, P. and W-P. Chen, 1982, "Seismicity and mountain building", in press.
- Parsons, B.E. and J.G. Sclater, 1977, "An analysis of the variation of ocean floor bathymetry and heat flow with age", *J. Geophys. Res.*, 82, 803-827.
- Sawyer, D.S., A. Swift, J.G. Sclater and M.N. Toksoz, 1981, "Extensional model for the subsidence of the northern United States Atlantic continental margin", *Geology*, 10, 134-140.
- Sclater, J.G. and P.A.F. Christie, 1980, "Continental stretching, an explanation of the post-Cretaceous subsidence of the central North Sea basin", *J. Geophys. Res.*, 85, 3711-3739.
- Sclater, J.G., L. Royden, F. Horvath, B.C. Burchfiel, S. Semken, and L. Stegena, 1980, "The formation of the Intra-Carpathian basins as determined from subsidence data", *Earth Planet. Sci. Lett.*, 51, 139-162.
- Stocker, R.L. and M.F. Ashby, 1973, "On the rheology of the upper mantle", *Rev. Geophys. and Space Phys.*, 11:2, 391-426.
- Vierbuchen, R.C., R.P. George and P.R. Vail, 1981, "A thermal-mechanical model of rifting with implications for outer highs on passive continental margins", in press.

Figure Captions

Figure 1. A strength profile for the lithosphere based on the assumption that the upper crust fails by frictional sliding on pre-existing fracture surfaces, the lower crust deforms according to the quartz flow law and the mantle deforms according to the olivine flow law.

Figure 2. Deformation map of olivine, showing the strength developed at each temperature as a function of strain rate. The heavy lines separate regions where different deformation mechanisms predominate.

Figure 3. Diagrammatic representation of the procedure involved in the modelling.

Figure 4. Diagram showing the system modelled. The two elements have uniform strengths B_1 and B_2 , and lengths L_1 and L_2 . The ends of the system are constrained to move apart at a constant velocity U_0 , and the upper and lower surfaces are free of shear stresses.

Figure 5. A typical strain-rate history for the model. The "basin" has strain rate $\dot{\epsilon}_2$ and the "continent" has strain rate $\dot{\epsilon}_1$. The intersection of the curves gives the time at which the "basin" and "continent" have the same strength.

Figure 6. A plot of the history of the ratio of lengths of the "continent" and "basin" during the extension. The "continent" is initially ten times as long as the "basin". The minimum value of $\frac{L_1}{L_2}$ occurs where $\dot{\epsilon}_1 = \dot{\epsilon}_2$ (see Fig. 5).

Figure 7. Contours of the value of β_2 when $\epsilon_1 = \epsilon_2$ for an initial strength ratio of 0.01 over a range of initial strain rates and values of Q/nRT_L . There is strong concentration of the strain in the basin for Q/nRT_L less than 2.5 over the whole range of initial strain rates.

For high Q/nRT_L , the extent of strain concentration depends upon the initial strain rate. In this figure, and in Figs. 8 and 9, the shaded area shows the region of parameter space for which stretching ceases after 0.04 DTU. Below this shaded area, stretching is possible for longer than 0.04 DTU.

Figure 8. Contours of the value of β_2 when $\dot{\epsilon}_1 = \dot{\epsilon}_2$ in $Q/nRT_L - \epsilon_0$ space for an initial strength ratio of 0.1. The disposition of β_2 contours is almost the same as in Fig. 6.

Figure 9. Contours of the value of β_2 when $\dot{\epsilon}_1 = \dot{\epsilon}_2$ in $Q/nRT_L - \dot{\epsilon}_0$ space for an initial strength ratio of 0.75. There is less strain concentration at low Q/nRT_L than in the two previous cases, and the range of β_2 values possible at high Q/nRT_L is more restricted.

Figure 10. A plot of stress in the "basin", relative to its initial value, for increasing strain in the "basin". After falling slightly, the stress increases very rapidly as the Moho temperature falls below some "threshold" temperature which depends on the value of Q/nRT_L .

Figure 11. A plot of the surface heat flux, relative to its initial value, with increasing strain for $n = 1$, $\dot{\epsilon} = 5, 50$ and 150 , and $Q/nRT_L = 1.5, 15, 40$. For a basin caused by instantaneous stretching, the maximum value of q/q_0 would lie on the $q/q_0 = \beta$ line. Clearly, for more realistic strain histories the peak value of q/q_0 is displaced from this line, especially for low values of Q/nRT_L . For Q/nRT_L , the peak value of q/q_0 is quite close to the $q/q_0 = \beta$ line.

Figure 12. As Fig. 11, but for $n = 3$. Again, for $Q/nRT_L = 40$ the maximum q/q_0 is quite close to the $q/q_0 = \beta$ line, whereas for lower Q/nRT_L , it is significantly displaced.

Figure 13. As Fig. 11, but for $n = 6$.

Figure 14. Density profiles through the lithosphere a) immediately after stretching and b) at equilibrium, after post-rift subsidence by an amount s . The lithosphere is now covered by an extra depth s of water and has a linear geotherm.

Table Captions

Table 1. Table of symbols used.

Table 2. This table gives, for an initial strength contrast of 0.1, and a variety of rheologies, the value of the maximum heat flux, the value of β_2 when this occurred, the predicted post rift subsidence, γ^* , the ratio of γ^* to $1-1/\beta$ (the amount of subsidence predicted by McKenzie's (1978) model), the stress in the system at the time of maximum heat flow, and the period of stretching in dimensionless time units (.04 DTU \approx 25 m.y.).

Table 1

θ	temperature
θ_0	surface temperature
θ_m	Moho temperature
T_0	initial Moho temperature
T_L	initial temperature of the base of the lithosphere
τ	deviatoric stress
σ_1, σ_3	greatest and least principal stresses
n	the "power law exponent" - a dimensionless number
Q	activation energy of the deformation mechanism
A, C, D, F	material constants
R	gas constant
$\dot{\epsilon}_p$ and σ_p	reference strain rate and stress (in the Dorn law)
$\dot{\epsilon}$	strain rate
$U_0, \dot{\epsilon}_0$	boundary velocity, and corresponding initial bulk strain-rate
d, a	lithospheric thickness, initial lithosphere thickness
B	lithosphere strength
T, \dot{E}	second invariants of the deviatoric stress, and strain-rate tensors
κ	thermal diffusivity
q	heat flow
q_0	equilibrium heat-flow
ρ_0	density of lithosphere material at 0°C
ρ_w	density of seawater
α	thermal expansivity of lithosphere material
s	amount of post-tectonic subsidence

Table 2

n	ϵ_0	Q/nRT_L	max. heat flux	β_2	γ^*	γ^*/γ	τ/τ_0	time to max. heat flux
1	5	1.5	1.3	2	.14	.28	0.49	>.09
		15	1.2	1.3	.10	.43	1.6	>.09
		40	1.1	1.2	.08	.47	1.7	.090
	50	1.5	2.6	4.1	.54	.71	0.16	.078
		15	2.3	2.8	.50	.78	1.5	.042
		40	1.9	2.0	.42	.84	1.7	.042
	150	1.5	3.8	6.0	.68	.82	0.10	.039
		15	3.5	4.3	.66	.86	1.4	.033
		40	3.1	3.3	.62	.88	1.7	.024
3	5	1.5	1.5	2.0	.20	.40	0.50	>.09
		15	1.4	1.6	.20	.53	4.5	>.09
		40	1.3	1.4	.18	.62	5.6	.072
	50	1.5	2.9	4.0	.56	.75	0.23	.060
		15	2.7	3.4	.56	.79	4.2	.051
		40	2.5	2.7	.54	.86	5.3	.036
	150	1.5	4.0	5.9	.70	.84	0.19	.033
		15	3.8	4.7	.67	.85	3.0	.027
		40	3.6	3.8	.64	.86	4.2	.021
6	5	1.5	1.5	2.0	.20	.40	0.56	>.09
		15	1.4	1.6	.20	.52	5.5	>.09
		40	1.3	1.4	.18	.62	6.2	.081
	50	1.5	2.9	4.0	.56	.75	0.28	.060
		15	2.8	3.4	.56	.79	7.7	.048
		40	2.5	2.7	.54	.86	7.9	.033
	150	1.5	4.1	6.0	.70	.84	0.35	.033
		15	3.9	4.8	.70	.88	10.2	.033
		40	3.5	3.8	.66	.89	10.3	.021

Figure 1

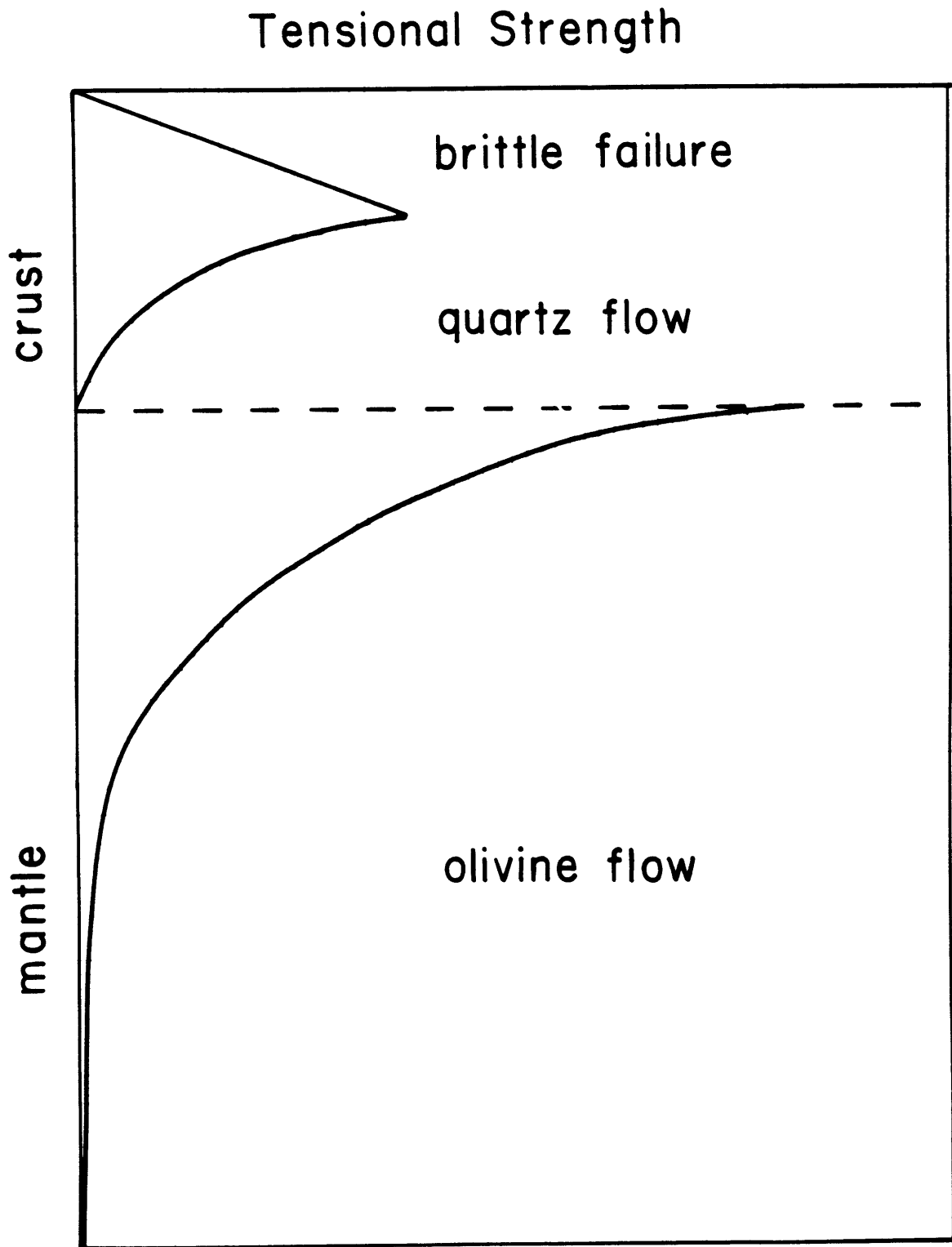


Figure 2

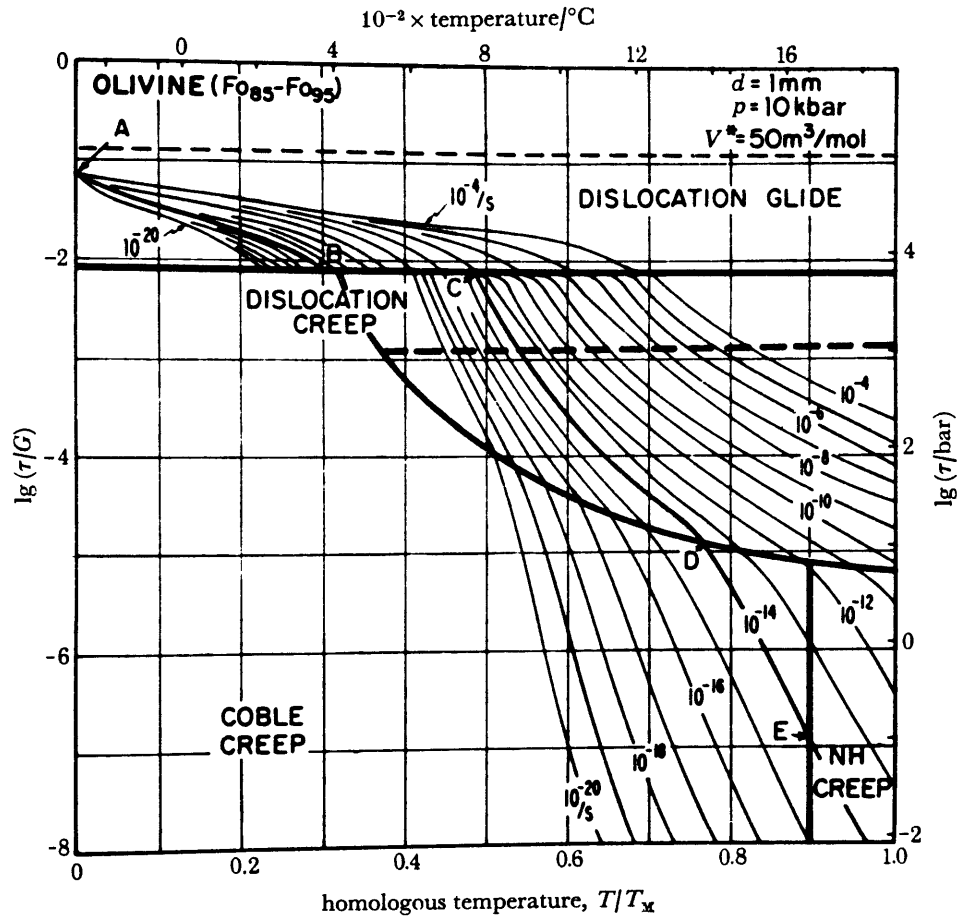


Figure 3

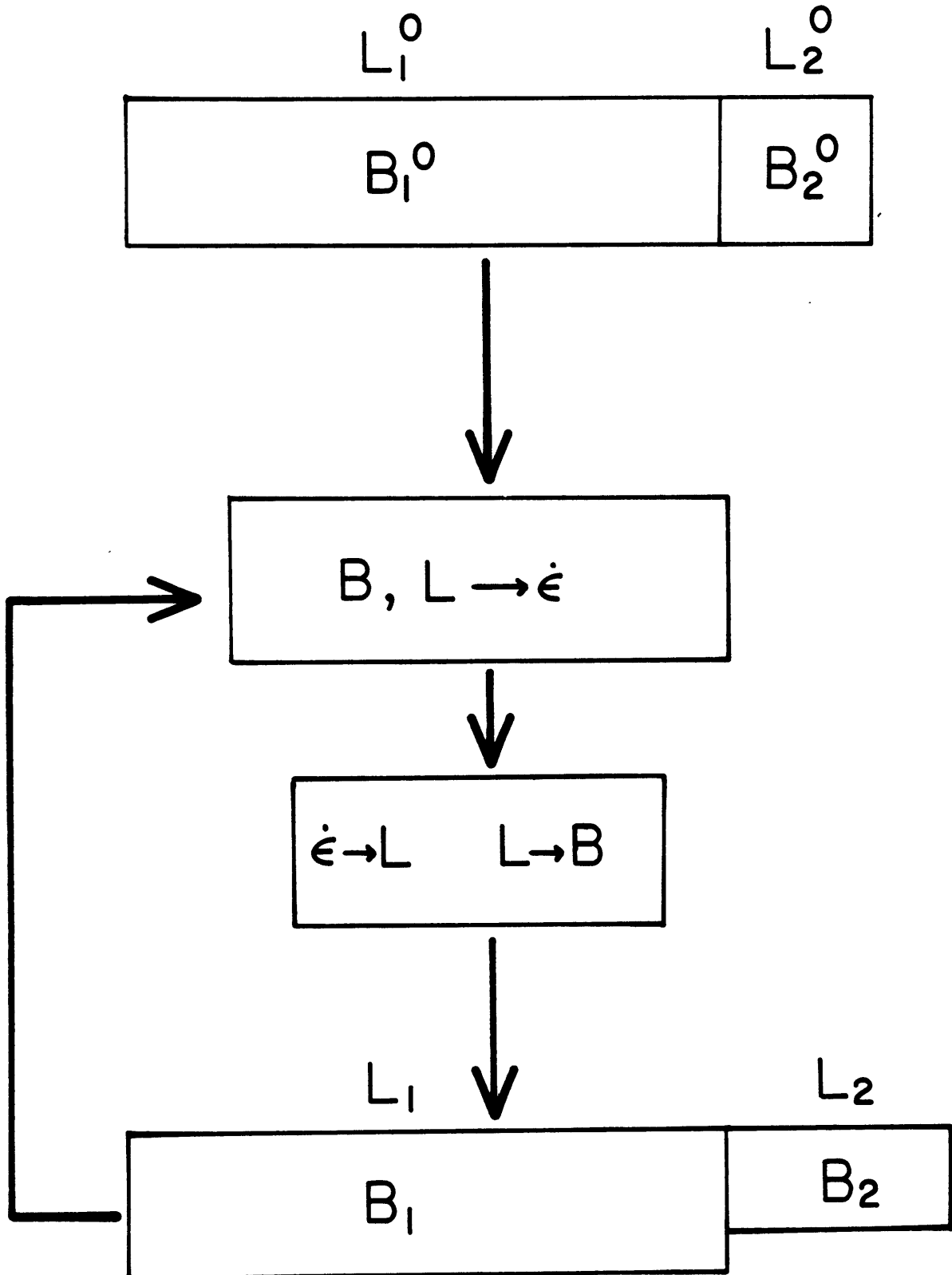


Figure 4

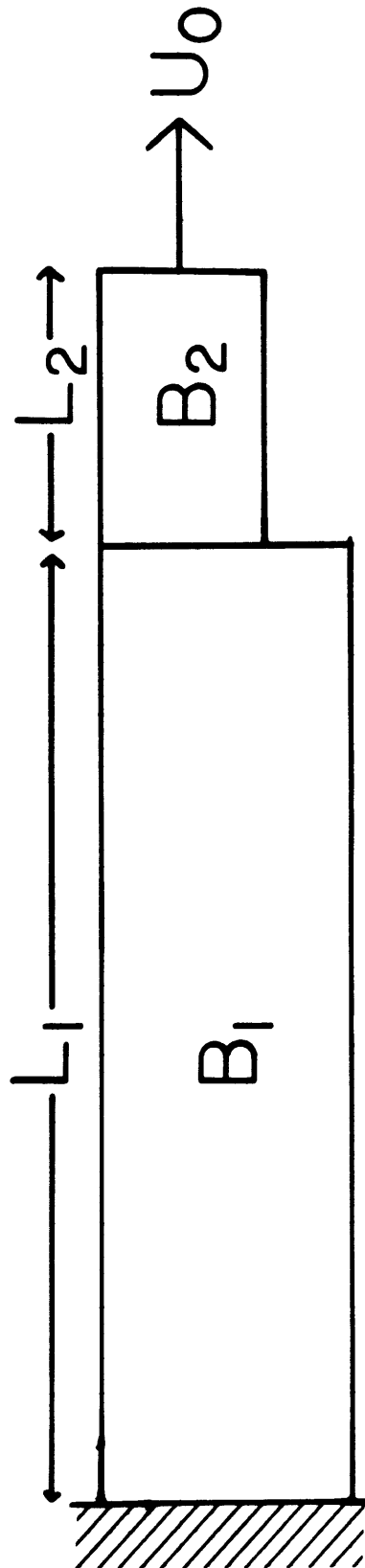


Figure 5

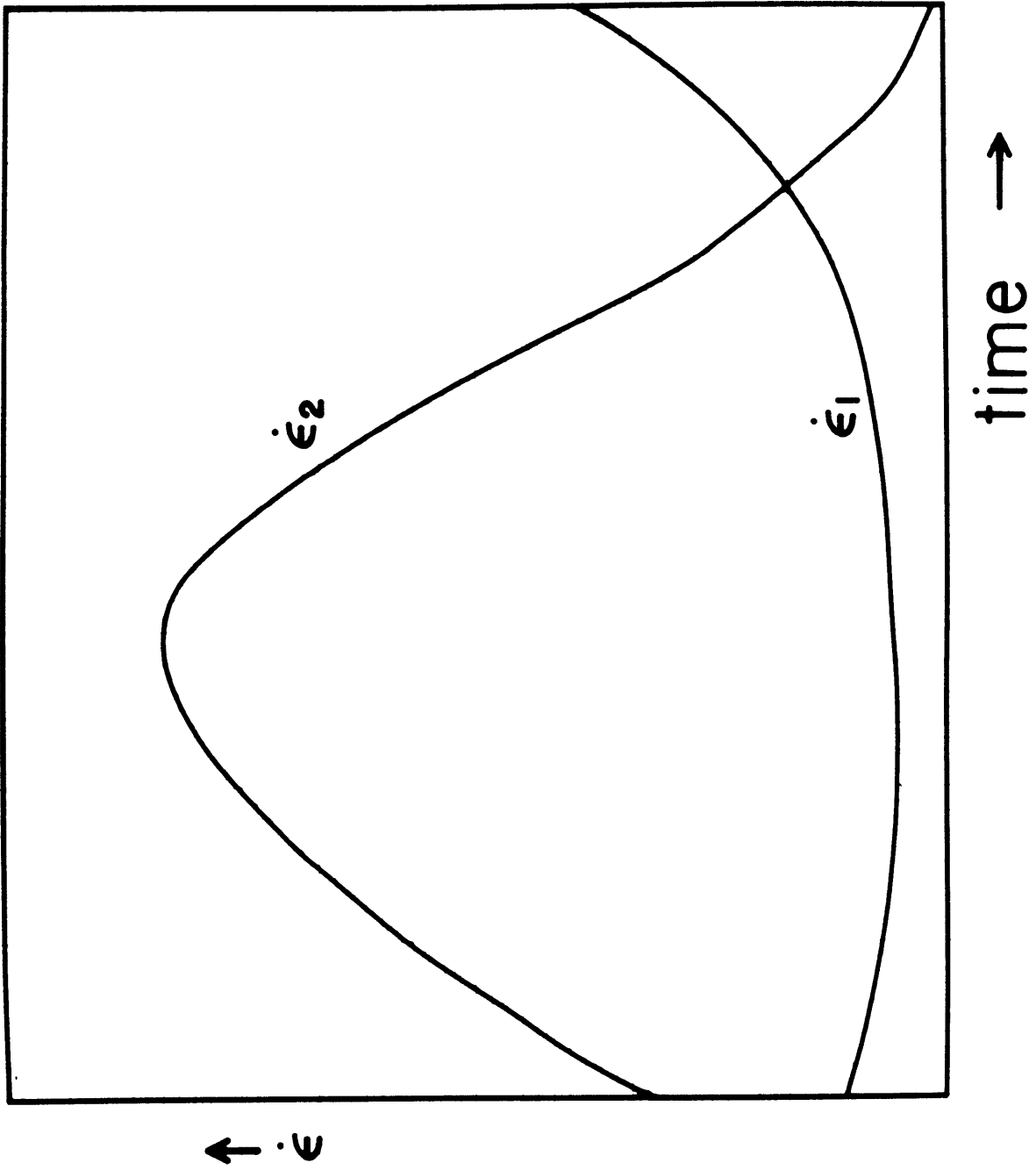
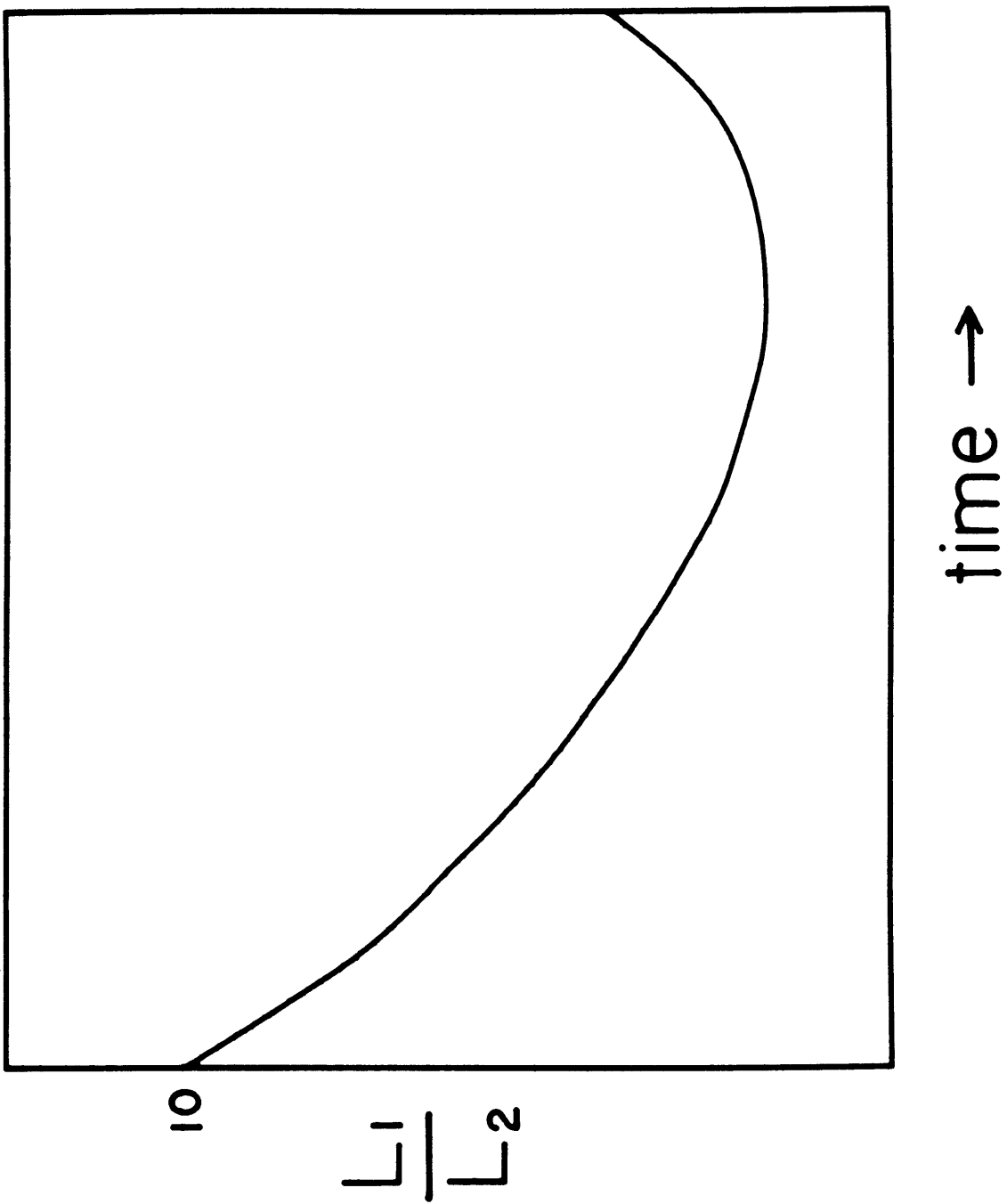


Figure 6



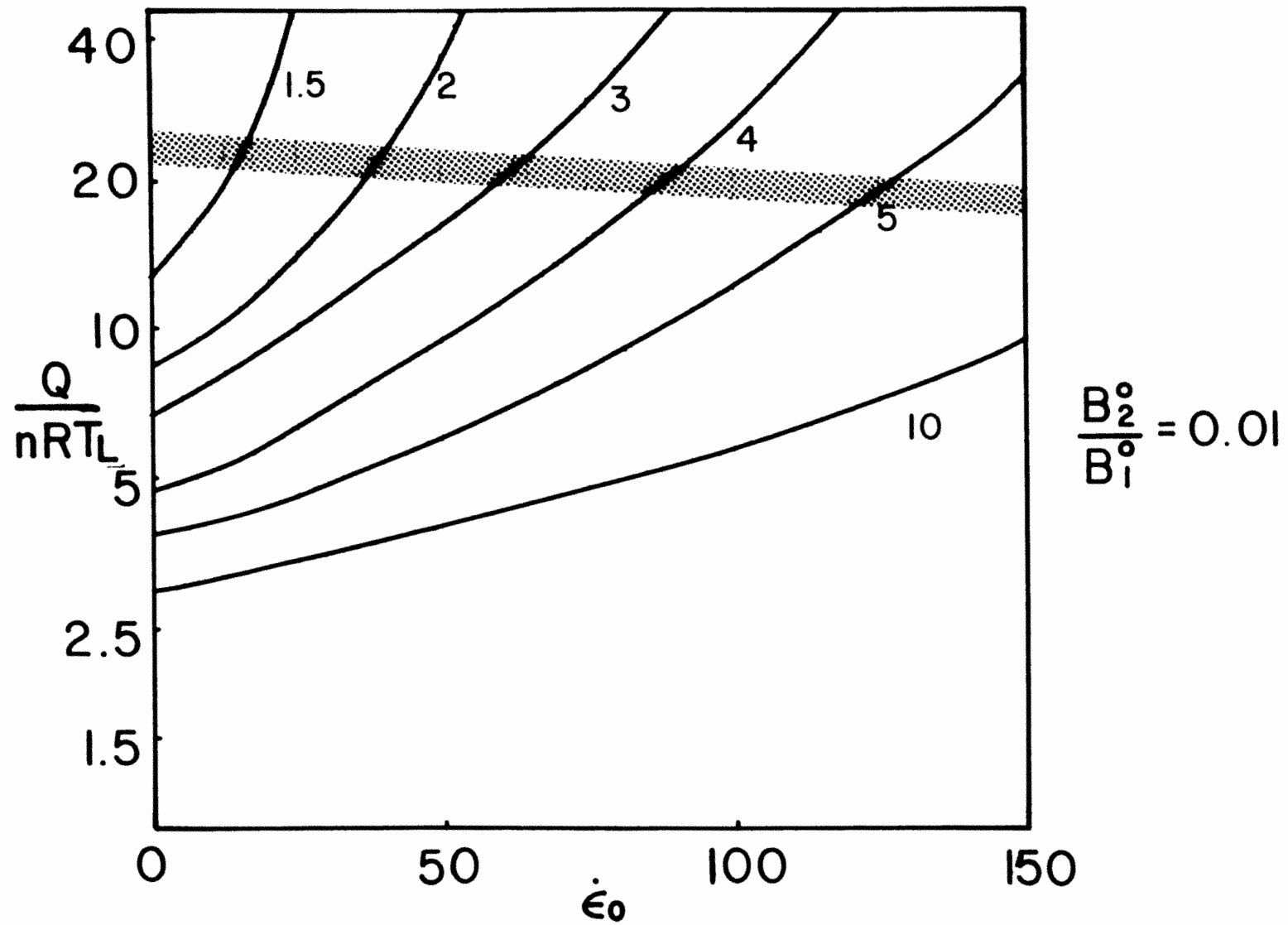
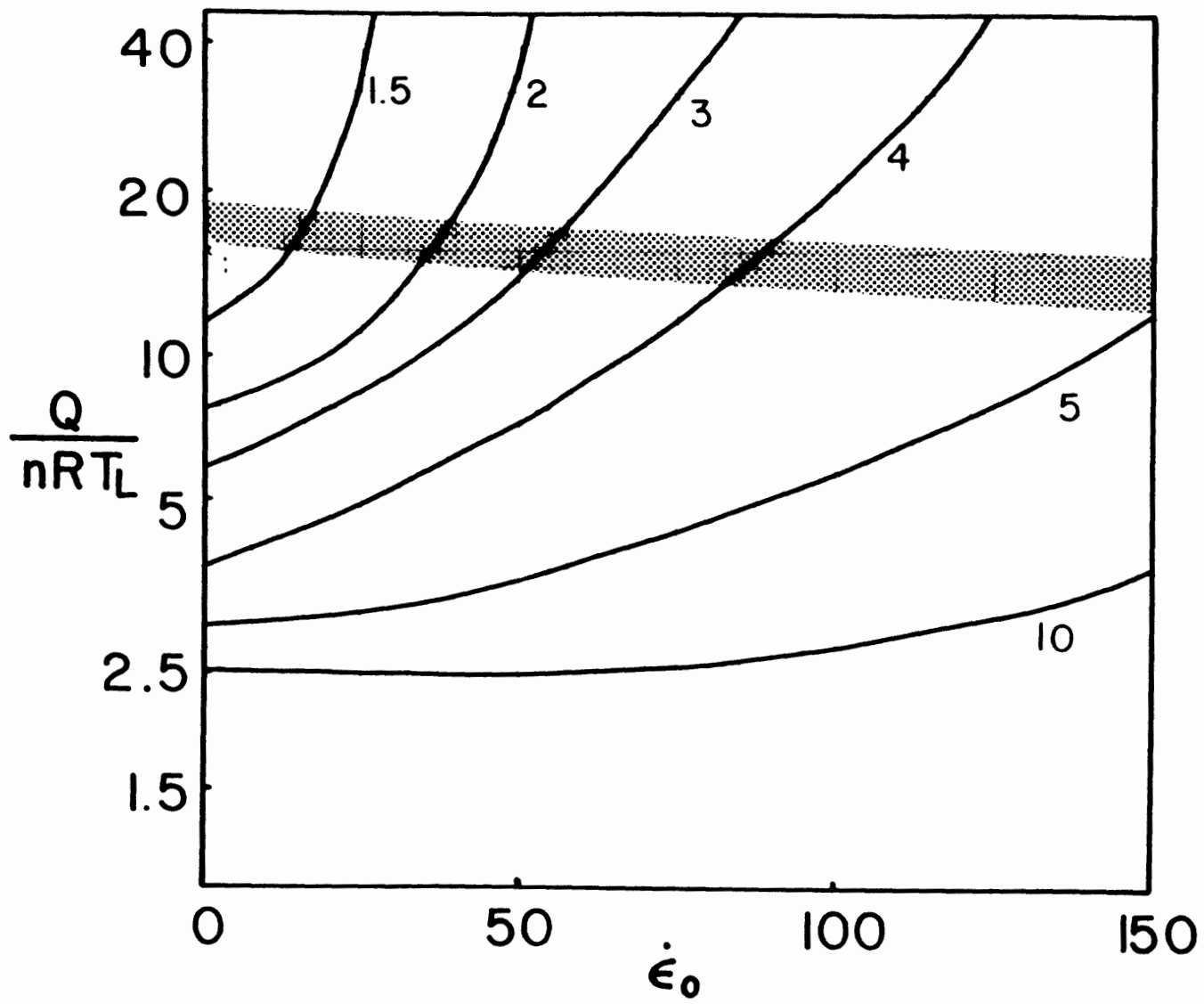
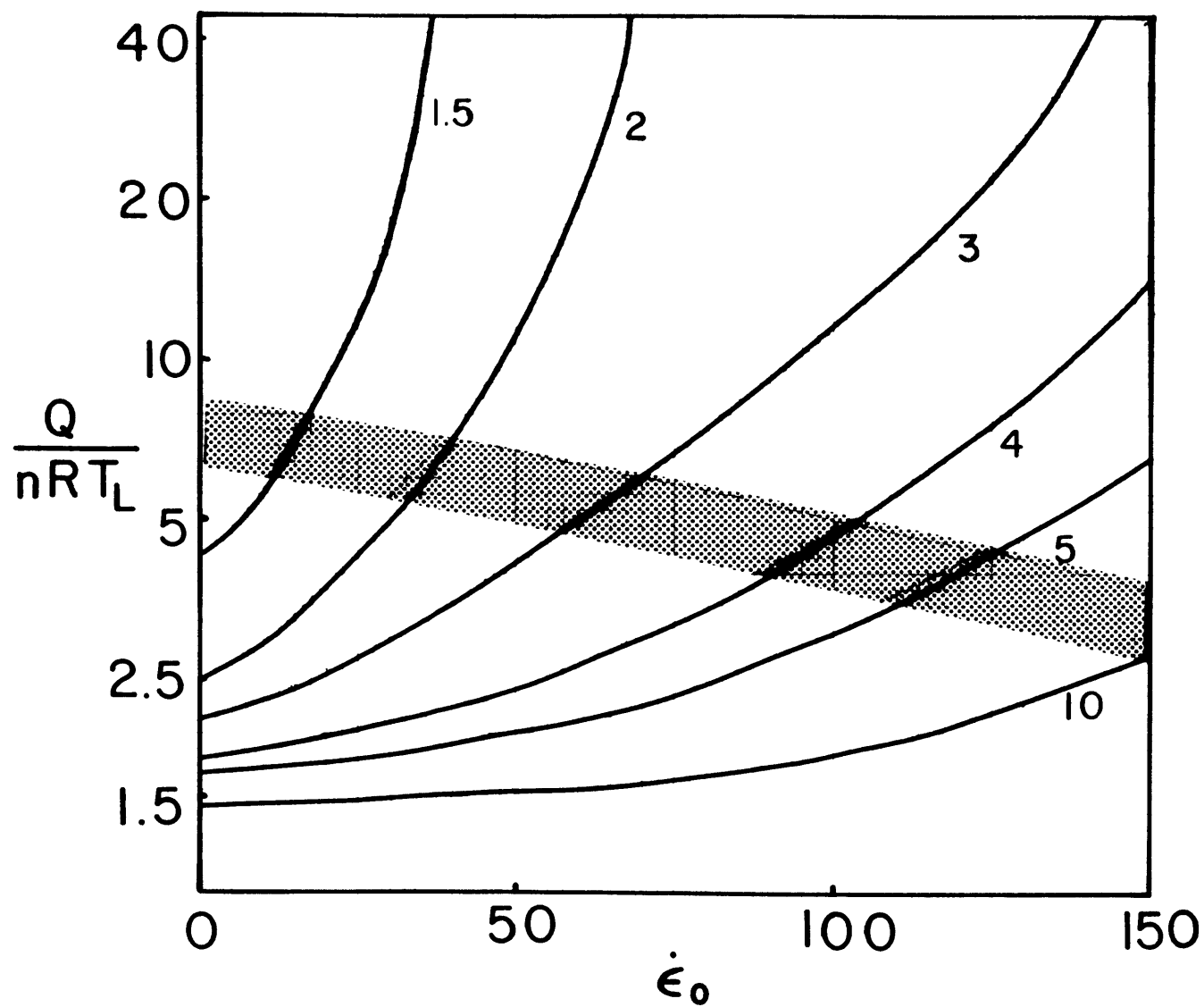


Figure 7



$$\frac{B_2^0}{B_1^0} = 0.1$$

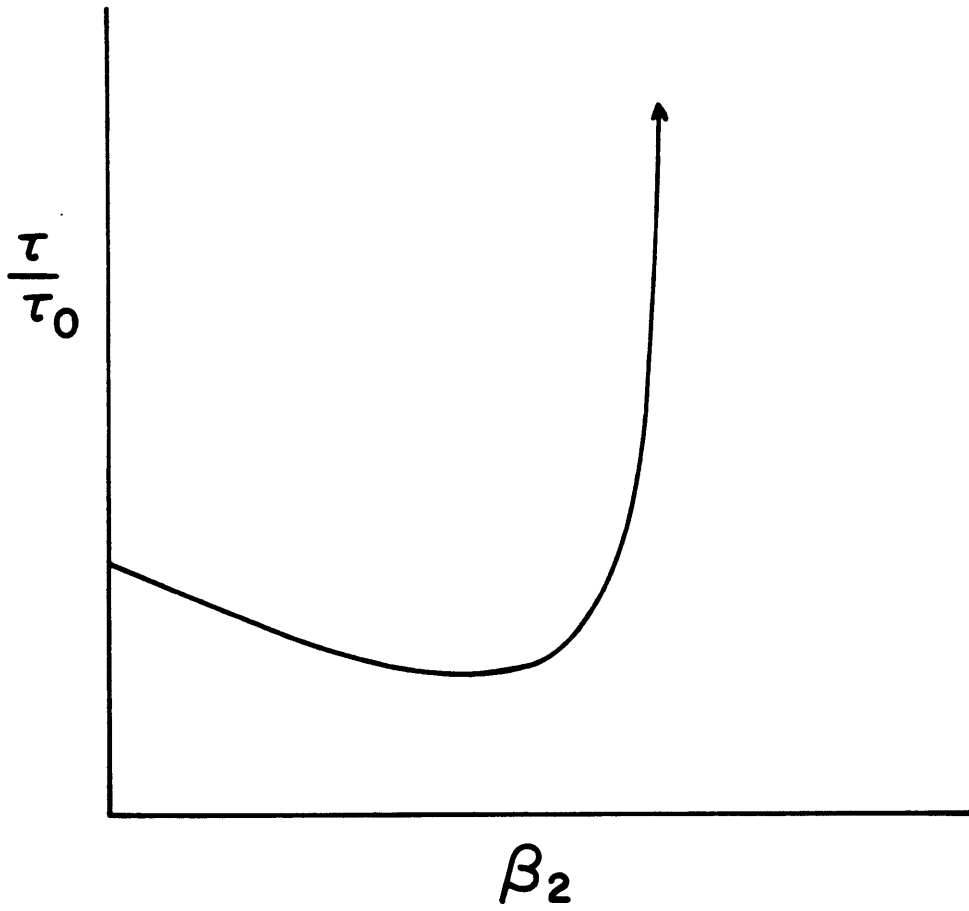
Figure 8



$$\frac{B_2^0}{B_1^0} = 0.75$$

Figure 9

Figure 10



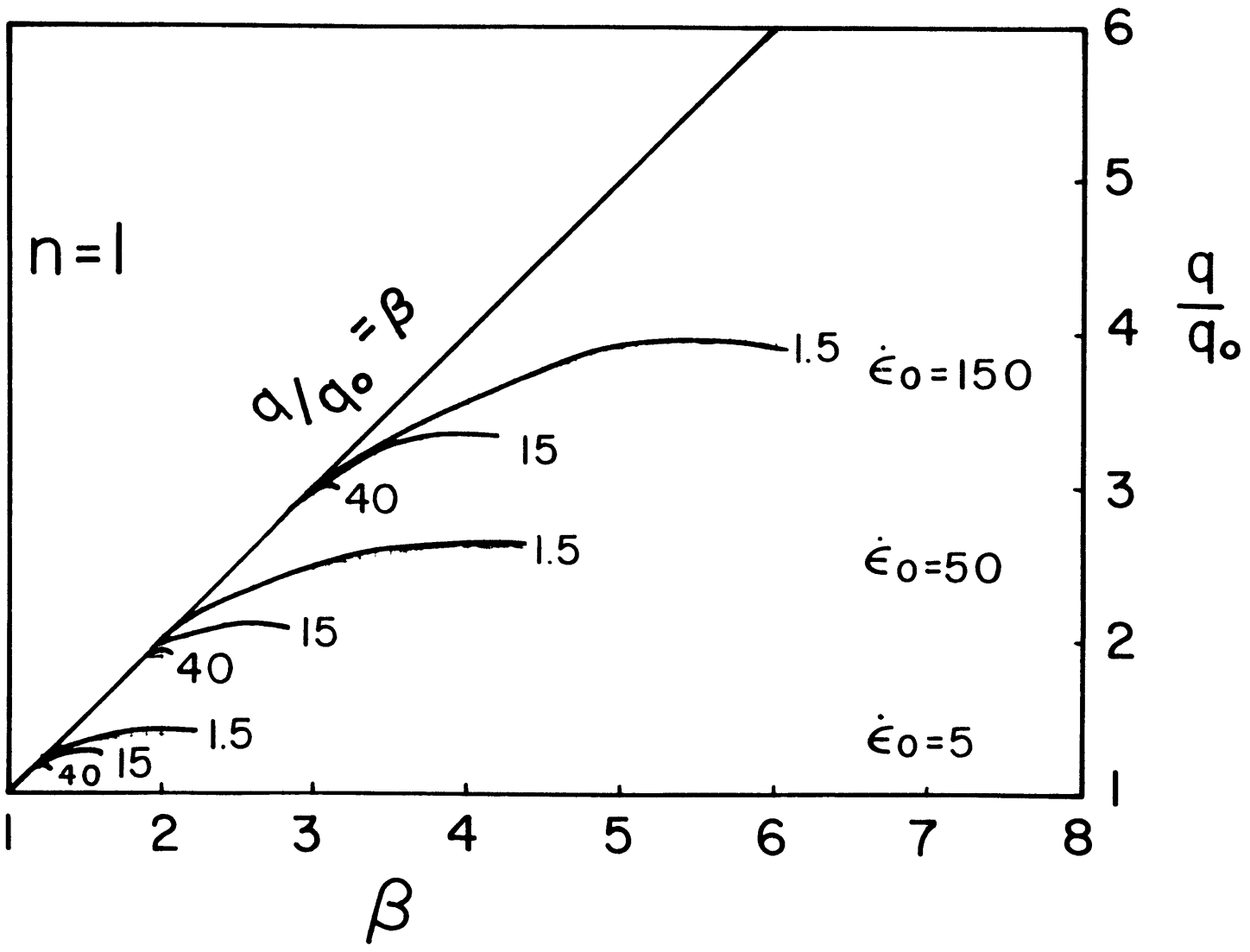


Figure 11

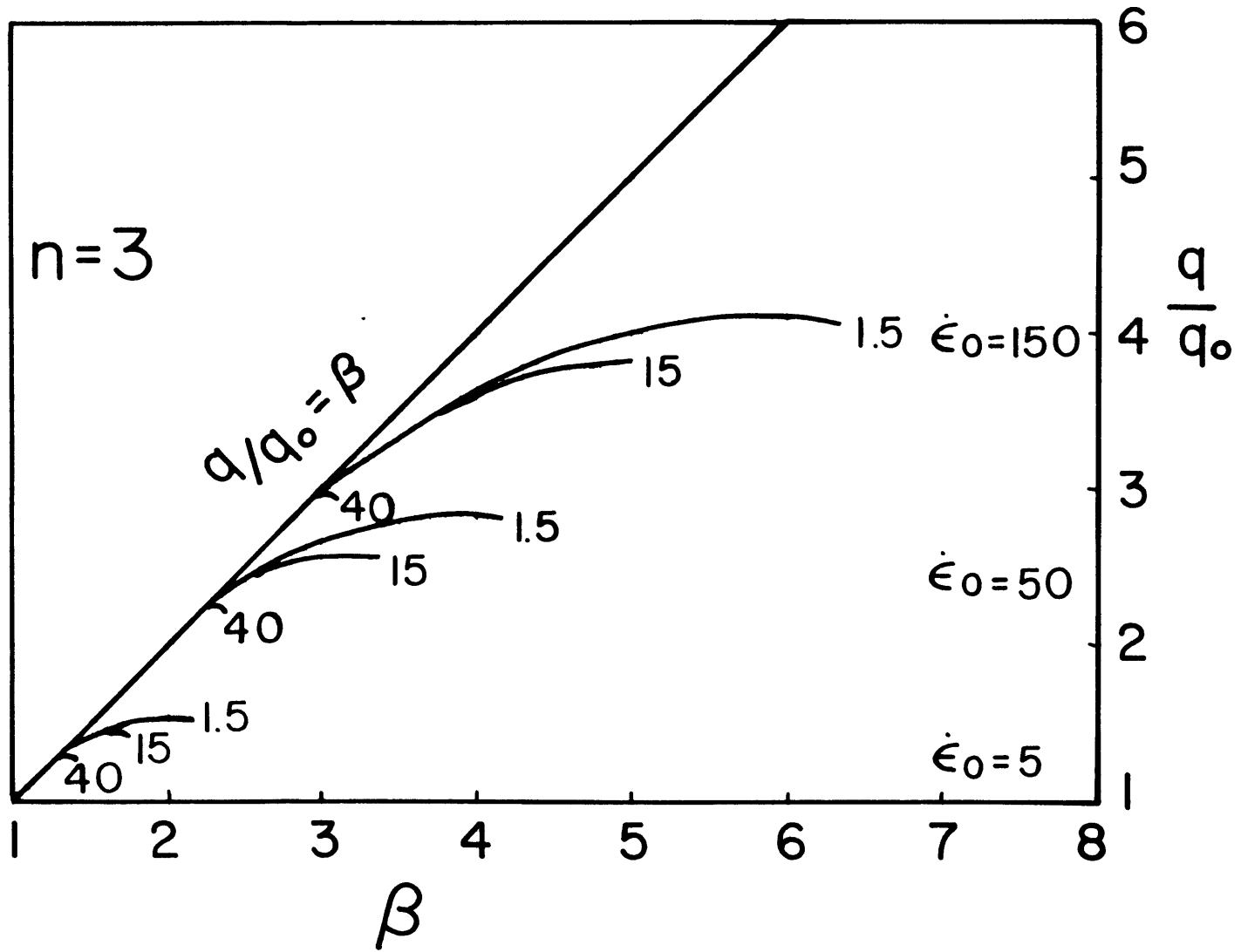
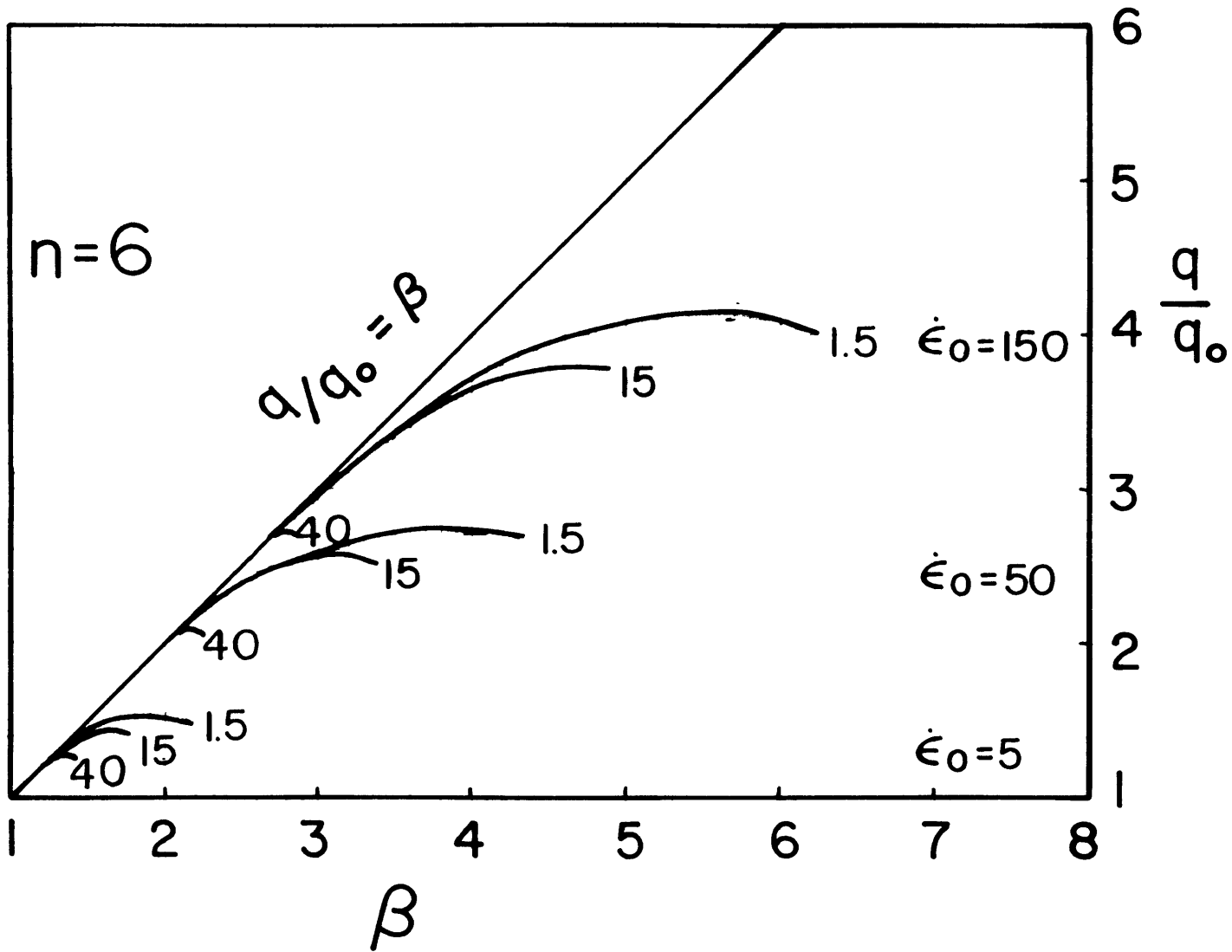


Figure 12



51
Figure 13

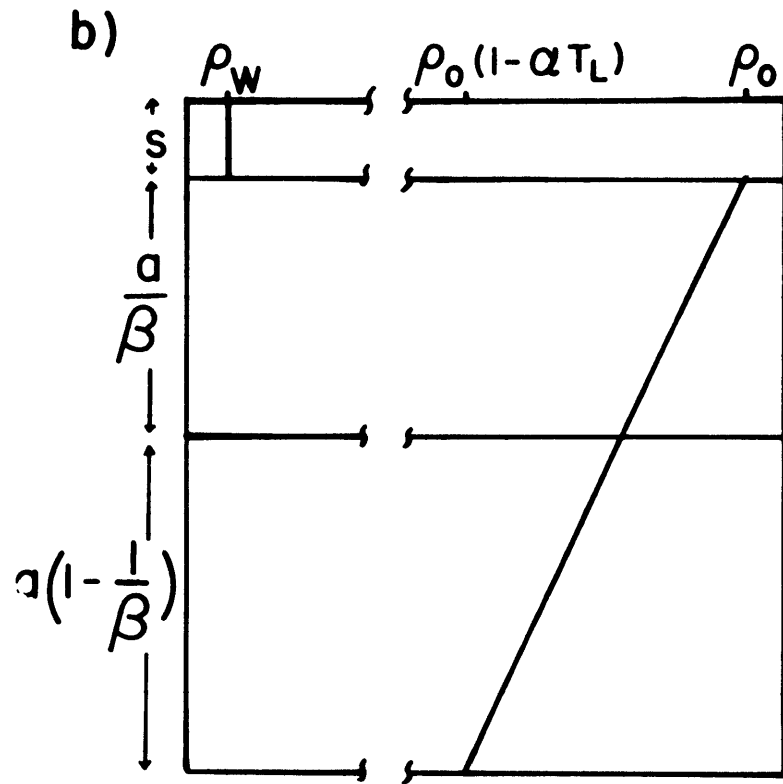
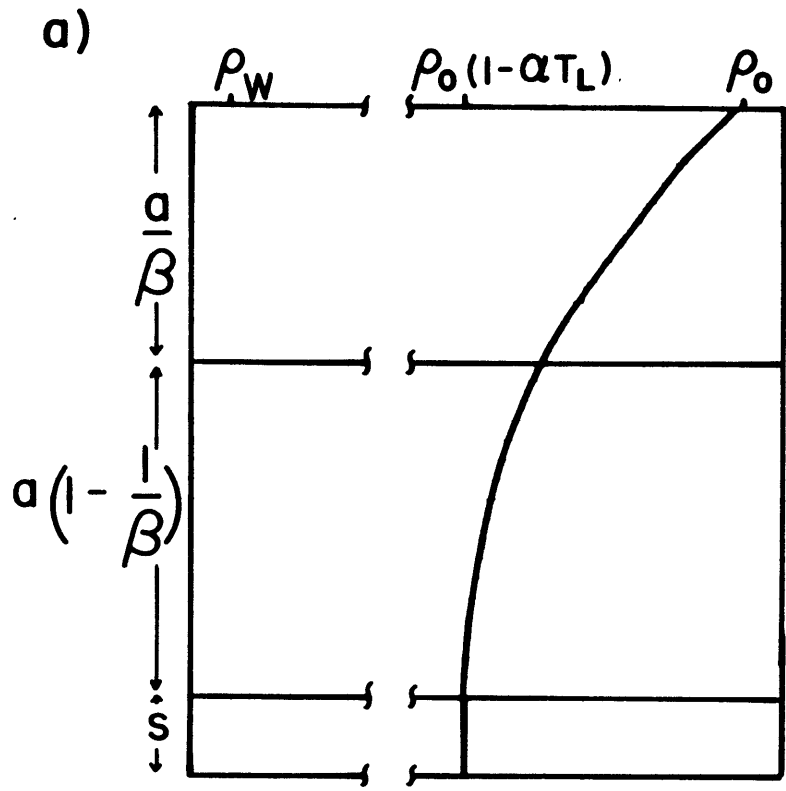


Figure 14